Journal of Advanced Scientific Research

Available online through http://www.sciensage.info

ISSN 0976-9595

Research Article

THEORETICAL AND SPECTROSCOPIC STUDIES ON 3- HYDROXY COUMARIN

E. Jayachithra*[1], R.Madivanane[2], R.Jayasheela[3], Periandy[3]

[1]*Department of Physics, Research and Development Center, Bharathiyar University, Coimbatore, Tamil Nadu, India*

[2]*Department of Physics, Bharathidasan Govt. College for Women, Puducherry, India*

[3]*Department of Physics, Kanchi Mamunivar Institute for Post graduate Studies and Research, Puducherry, India*

**Corresponding author: jc.chitraphy@gmail.com*

ABSTRACT

In this present study, spectroscopic and computational work of 3-hydroxy coumarin were carried by density functional theory (DFT) methods with B3LYP functionals and 6-311++G (d, p) basis sets. FT-IR and FT-Raman spectrum was recorded in the region of 4000-500 cm^{-1} for the title molecule. The vibrational state of the molecules was calculated by DFT method and the theoretical vibrational wavenumbers were scaled by scaling factors and compared with the experimental results. NMR and UV spectra were recorded in both gas phase and solvent phase with same combination of basis sets. The anti-bacterial activity of this molecule was studied using molecular docking.

Keywords: 3-Hydroxy coumarin, FT-IR and FT-Raman, NMR, UV-Vis, DFT, Docking.

1. INTRODUCTION

Coumarins are natural and synthetic compound exhibit wide biochemical and pharmacological activities including antioxidant, anti- inflammatory, anti-cancer and even enzyme inhibitors [1-2]. The Coumarin compounds show excellent physical, chemical, optical and thermal properties which can be used as dyes for coloring fabrics, fluorophores and as optical brightening agents [3-4]. Due to their versatility and high bioactivities of Coumarins, these compounds attract the attention of many researchers. Chemically, a Coumarin shares C=C in the lactone with other organic motifs. The fused heterocycle is beneficial for transferring electrons, and the abundance of these electrons makes the molecule as potential antioxidants. However, the presence of appropriate substituent groups on aromatic rings can modify the molecular electron distribution, leading to new agents with high potential bioactivity [5]. Therefore, methods for obtaining and characterizing new Coumarins and derivatives have been widely studied.

Among the family of Coumarins, 3-hydroxylCoumarin, a derivative with hydroxyl group at the 3-postion, have been extensively studied for their wide range of biological activities such as antioxidant, that provides protection against oxidative degradation of foods and plays an important role in the treatment of many chronic diseases, such as atherosclerosis, brain dysfunction, immune system decline and also cancer [6]. These special applications of 3- hydroxyl Coumarin (3HC) has motivated considerable interest to study the structural information combined with computational methods to investigate the physical and chemical properties. Literature survey reveals that no *ab initio* DFT with 6-311++G(d,p) basis set calculations of 3-hydroxycoumarin (3HC) has been reported so far. It is, therefore thought worthwhile to make a comprehensive spectral analysis using both experimentally and theoretically.

The present work describes the vibrational spectral investigations of 3HC aided by density functional computations to elucidate the correlation between the molecular structure and biological activity, bonding features, electron delocalization, and the intra molecular charge transfer interactions and molecular docking. Furthermore, vibrational spectra were interpreted in terms of total energy distributions (TEDs) and the assignments of the experimental bands were made.

2. EXPERIMENTAL

The sample 3HC was procured from reputed sigma-Aldrich chemicals Ltd and used as such for recording the spectra. The FTIR spectrum of the compound are recorded over the region on 4000-400 cm^{-1} at a resolution of ± 0.1 cm^{-1} using Thermo Nicolet-6700 Fourier transform spectrometer, and UV-Visible spectral measurements have been made using Shimadzu spectrophotometer in the wavelength region 200-400 nm

at Pondicherry university. All sharp bands observed in the spectra are expected to have an accuracy of ±1 cm^{-1}. The FT Raman spectrum is analyzed in the range 50-3500 cm^{-1} at BRUKER IFS-66Vmodel interferometer equipped with an FRA-106 FT-Raman accessory.

2.1. Computational details

The quantum chemical calculations of 3HC have been performed on DFT (B3LYP) methods with 6-311++ G(d,p) basis sets using the Gaussian 09W program [7]. The optimized structural parameters have been evaluated for the calculations of vibrational frequencies. After scaled with the scaling factor, the deviation from the experiments is less than 10 cm^{-1} with a few exceptions. The assignments of the calculated normal modes have been made on the basis of the corresponding PEDs.

The PEDs are computed for vibrational frequencies using VEDA program [8]. Gaussview Program [9] has been used to get visual animation and for the verification of the normal modes assignment. The accuracy and reliability of DFT/B3LYP functional was shown in computing various molecular properties such as nonlinear optical properties, HOMO-LUMO energies etc. of organic systems. For these reasons optical band gap (HOMO-LUMO) of minimum energy conformer is calculated with DFT method at B3LYP/6-311++ (d,p) [10] level of theory using the Gaussian 09W software [7]. MEP analysis have been made using DFT/B3LYP method with 6-311++G (d,p) basis set.

The electronic absorption spectra for optimized molecule calculated with the time dependent DFT (TD-DFT) at B3LYP/6-311++G (d,p) level in gas phase and solvent (DMSO and chloroform). The ^{13}C and ^{1}H nuclear magnetic resonance (NMR) chemical shifts of the molecule were calculated by the gauge independent atomic orbital (GIAO) method in chloroform and compared with experimental results.

3. RESULT AND DISCUSSION

3.1. Molecular Analysis

The molecular structure of 3HC belongs to C1 point group symmetry. The optimized molecular structure of the title molecule is shown in fig. 1 was obtained using GAUSSIAN 09 program. The optimized bond lengths, bond angles and torsional angles are listed in table 1. The calculated energy of DFT method is greater method because the assumption of ground state energy corresponding to the true energy.

The structural analysis shows that there is a drastic change in the C-C bond length values inside the pyrone ring, whereas it remains almost the same in phenyl ring The CC bonds inside the phenyl ring C3-C4, C3-C8, C4-C9, C8-C11, C9-C10 and C10-C11 are found to have values 1.400, 1.400, 1.390, 1.385, 1.389 and 1.400 Å, respectively. All these values are closer to the expected values 1.38 or 1.39Å for pure benzene, which shows the influence of the pyrone ring and OH groups are minimal on this ring. Whereas the inside the pyrone ring, C1-C2 is 1.351Å, this is almost a double bond, the C1-C5 is 1.468Å and C2-C3 1.439Å, and these are almost single bond values. All these three CC bond values indicate there is no conjugation inside the pyrone ring, as it is usually found in the phenyl ring, due to the presence on O atom inside the ring. The two CO values outside the pyrone ring; C1-O17is 1.34 Å and C5=O16 is 1.211 Å, the first one is clearly a single bond while the second one is a double bond. The two CO bonds inside the pyrone ring C4-O15 is1.377 Å and C5-O151.360Å, which shows variation among them as well as with the bond outside the ring. That shows there is a kind of sharing of electrons from the CC bonds to CO bonds inside the ring [11]. The C-H bond length in the benzene ring are same *i.e.,* 1.08Å. The O-H bond length in the pyrone ring is 0.977Å, which is due to the electro negativity of the oxygen atom. All the C-C bond length is almost in the range 1.35 to 1.46Å. The global minimum energy is obtained by DFT/B3LYP level using 6-311++G (d,p) basis set for the title molecule are 721.2539 a.u respectively.

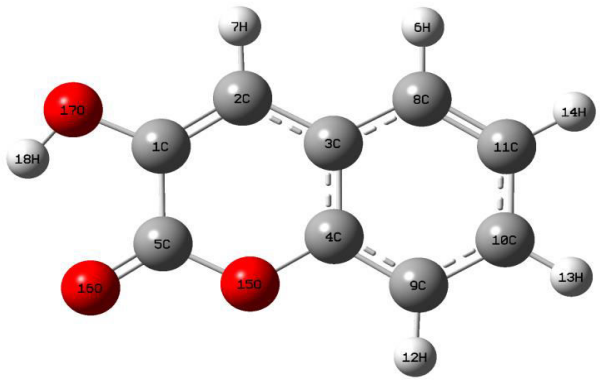

Fig. 1: Molecular structure of 3-hydroxy Coumarin

Table 1: Optimized Geometrical parameter for 3-hydroxy coumarin Computed at B3LYP/6-311++G (d, p)

Bond length (Å)		Bond Angle (°)		Dihedral angle(°)	
C1-C2	1.3511	C2-C1-C5	121.3231	C5-C1-C2-C3	-0.0034
C1-C5	1.4687	C2-C1-O17	123.6541	C5-C1-C2-H7	180.0049
C1-O17	1.3483	C5-C1-O17	115.0228	O17-C1-C2-C3	179.9948
C2-C3	1.4394	C1-C2-C3	119.5888	O17-C1-C2-H7	0.0031
C2-H7	1.0839	C1-C2-H7	120.2309	C2-C1-C5-O15	-0.0035
C3-C4	1.4045	C3-C2-H7	120.1803	C2-C1-C5-O16	-179.9918
C3-C8	1.407	C2-C3-C4	118.5139	O17-C1-C5-O15	-180.0018
C4-C9	1.3907	C2-C3-C8	123.7814	O17-C1-C5-O16	0.0098
C4-O15	1.377	C4-C3-C8	117.7047	C2-C1-O17-H18	180.0327
C5-O15	1.3606	C3-C4-C9	122.125	C5-C1-O17-H18	0.031
C5=O16	1.2115	C3-C4-O15	120.7883	C1-C2-C3-C4	0.0005
H6-C8	1.0844	C9-C4-O15	117.0867	C1-C2-C3-C8	-179.9835
C8-C11	1.3859	C1-C5-O15	117.3934	H7-C2-C3-C4	-180.0078
C9-C10	1.3892	C1-C5-O16	122.2013	H7-C2-C3-C8	0.0082
C9-H12	1.0828	O15-C5-O16	120.4053	C2-C3-C4-C9	-180.0006
C10-C11	1.4003	C3-C8-H6	118.8387	C2-C3-C4-O15	0.0095
C10-H13	1.0835	C3-C8-C11	120.7404	C8-C3-C4-C9	-0.0156
C11-H14	1.0835	H6-C8-C11	120.4209	C8-C3-C4-O15	179.9945
O17-H18	0.9722	C4-C9-C10	118.9019	C2-C3-C8-C11	0.0055
		C4-C9-CH12	119.1694	C2-C3-C8-C11	179.9975
		C10-C9-H12	121.9287	C4-C3-C8-H6	180.0214
		C9-C10-C11	120.3456	C4-C3-C8-C11	0.0133
		C9-C10-H13	119.5712	C3-C4-C9-C10	0.0061
		C11-C10-H13	120.0833	C3-C4-C9-H12	-179.9876
		C8-C11-C10	120.1824	O15-C4-C9-C10	179.9964
		C8-C11-H14	119.8876	O15-C4-C9-H12	0.0027
		C10-C11-H14	119.93	C3-C4-O15-C5	-0.0172
		C4-O15-C5	122.3924	C9-C4-O15-C5	179.9924
		C1-O17-H18	106.7225	C1-C5-O15-C4	0.0138
				O16-C5-O15-C4	-179.9976
				C3-C8-C11-C10	-0.0019
				C3-C8-C11-H14	180.0058
				H6-C8-C11-C10	-180.0101
				H6-C8-C11-H14	-0.0024
				C4-C9-C10-C11	0.006
				C4-C9-C10-H13	-179.9942
				H12-C9-C10-C11	-180.0006
				H12-C9-C10-H13	-0.0008
				C9-C10-C11-C8	-0.008
				C9-C10-C11-H14	179.9843
				H13-C10-C11-C8	179.9922
				H13-C10-C11-H14	-0.0155

3.2. Mulliken & Natural Charge analysis

Atomic charge analysis [12] is the key function for quantum chemical calculations of molecular systems because atomic charges influence the molecular system properties via dipole moment, polarizability etc. The atomic charges were calculated by B3LYP functionals and 6-311++G (d,p) basis set. The atomic charges of the title molecule are presented in table 2 and in terms of the graphical representation is shown in fig. 2.

From charge analysis, it is observed that, in benzene ring, all carbon atoms have almost negative charges and they are ready to interact with the positive charge acceptors. The carbon atom C4 has high atomic charge prediction in Mullikan (-2.052) due to presence of

Oxygen atom (O15) in that location and C3 carbon atom contribute the higher negative atomic charge due to the attachment of C4 with oxygen atom. But in case of Natural atomic charge, all carbon atoms have almost equal negative charges and they are responsible for electrophilic attack sites. And all hydrogen atoms present in title compound have similar positive charges in both Mullikan and Atomic charge analysis.

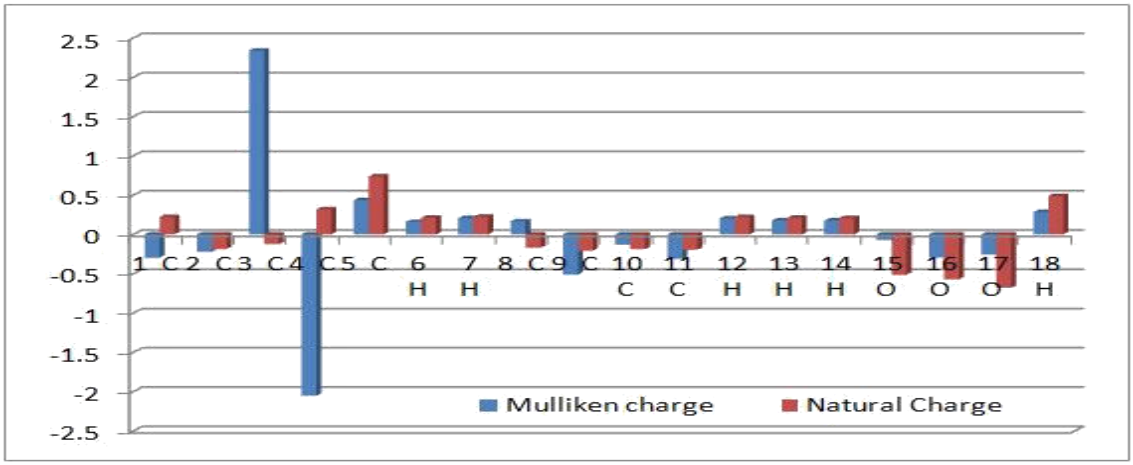

Fig. 2: Charge analysis of 3-hydroxy coumarin

Table 2: Mulliken and Natural Charge analysis of 3-hydroxy coumarin using B3LYP/6-311++G (d,p)

Atoms	Mulliken Charge Analysis	Natural Charge Analysis	Atoms	Mulliken Charge Analysis	Natural Charge Analysis
1 C	-0.29671	0.22054	11 C	-0.30861	-0.19632
2 C	-0.22194	-0.18536	12 H	0.20368	0.22118
3 C	2.33817	-0.12402	13 H	0.17736	0.21037
4 C	-2.05261	0.31732	14 H	0.17591	0.20827
5 C	0.43468	0.73875	15 O	-0.07054	-0.51493
6 H	0.15796	0.21012	16 O	-0.29402	-0.57189
7 H	0.20618	0.22358	17 O	-0.25663	-0.68039
8 C	0.16648	-0.17142	18 H	0.28436	0.48672
9 C	-0.51358	-0.20641			
10 C	-0.13029	-0.18614			

3.3. NMR Analysis

The NMR chemical shifts are sensitive to intermolecular interactions in the aqueous solution as compared to other heavier atoms [13]. For reliable calculations of magnetic properties accurate predictions of molecular geometry is very important. So, the shifts were determined with B3LYP/6-311++ (d,p) along with Gauge independent atomic orbital (GIAO) functional, in $CDCL_3$ in solvent phase, as the experimental shifts are determined in this phase. The shift values both experimental and theoretical are listed in table 3. The corresponding NMR Spectra in gas and solvent phase are depicted in fig. 3.

The carbon atoms in the phenyl ring are expected to give signal in between 120 -130 ppm [14] because of the equal negative charge distribution among them. This observation is made in all carbon atoms in the phenyl ring except 4C which is in contact of O atom of the pyrone ring. The 1C and 5C values in the pyrone ring are very much greater than the expected values, which is naturally due to presence of O atoms in the neighborhood. Thus it is clear that the conjugation of electrons is not uniform within this pyrone ring which deviates much in the region 1C-5C.

The chemical shift values for H atoms attached to benzene ring are expected between 7-8 ppm. Here for all the H atoms these values are observed, the values are 7.5, 7.1, 7.5, 7.6 and 7.4 ppm, all these values are in excepted line with a small variation. Only one H atom shows a very low value shift at 5.9 ppm which may be due to the intermolecular hydrogen bonds present at this site. These observations show the even the pyrone ring conjugation is closer to that of phenyl ring.

Table 3: 13C and 1H NMR analysis of 3-hydroxy Coumarin

Atom	Chemical shift	Experimental shift (ppm)
	Gasphase 6311G(2d,p)	Solvent phase $CDCl_3$ 6-311G(2d,p)
Carbon		
1C	146.9	146.2	149.44
2C	116.7	119.1	120.50
3C	129.6	129.1	128.51
4C	163.5	156.8	160.65
5C	163.5	164.5	160.65
8C	129.6	130.6	126.77
9C	121.1	121.2	120.50
10C	132.4	133.5	128.51
11C	129.6	130.1	128.51
Hydrogen			
6H	7.3	7.5	7.33
7H	6.9	7.1	7.1
12H	7.4	7.5	7.33
13H	7.4	7.6	7.34
14H	7.2	7.4	7.33
18H	5.8	5.9	6.40

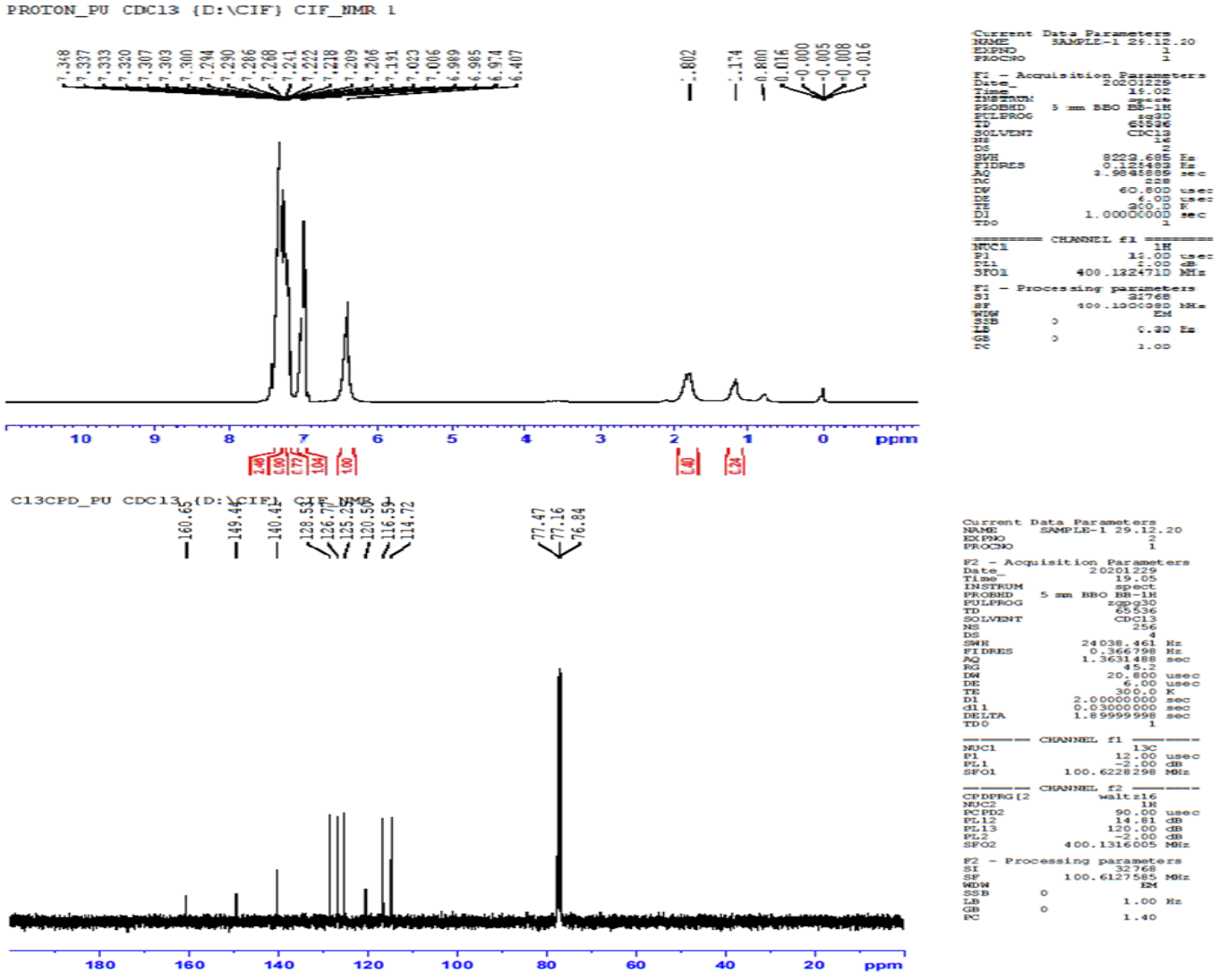

Fig. 3: ^{1}H and ^{13}C NMR Chemical shift of 3-hydroxy Coumarin

3.4. Vibrational Analysis

The title molecule 3-hydroxy coumarin belongs to C1point group symmetry. It has 18 atoms and 48 possible modes of vibrations [15]. All these modes of vibrations are observed collectively in both FT-IR and FT-Raman spectra. The wavenumbers are calculated and compared with the experimental one to assign the vibrational modes of the molecule which are presented in table 4. The experimental and theoretical FT-IR and FT-Raman spectra of the molecule are depicted in fig. 4 and 5 respectively.

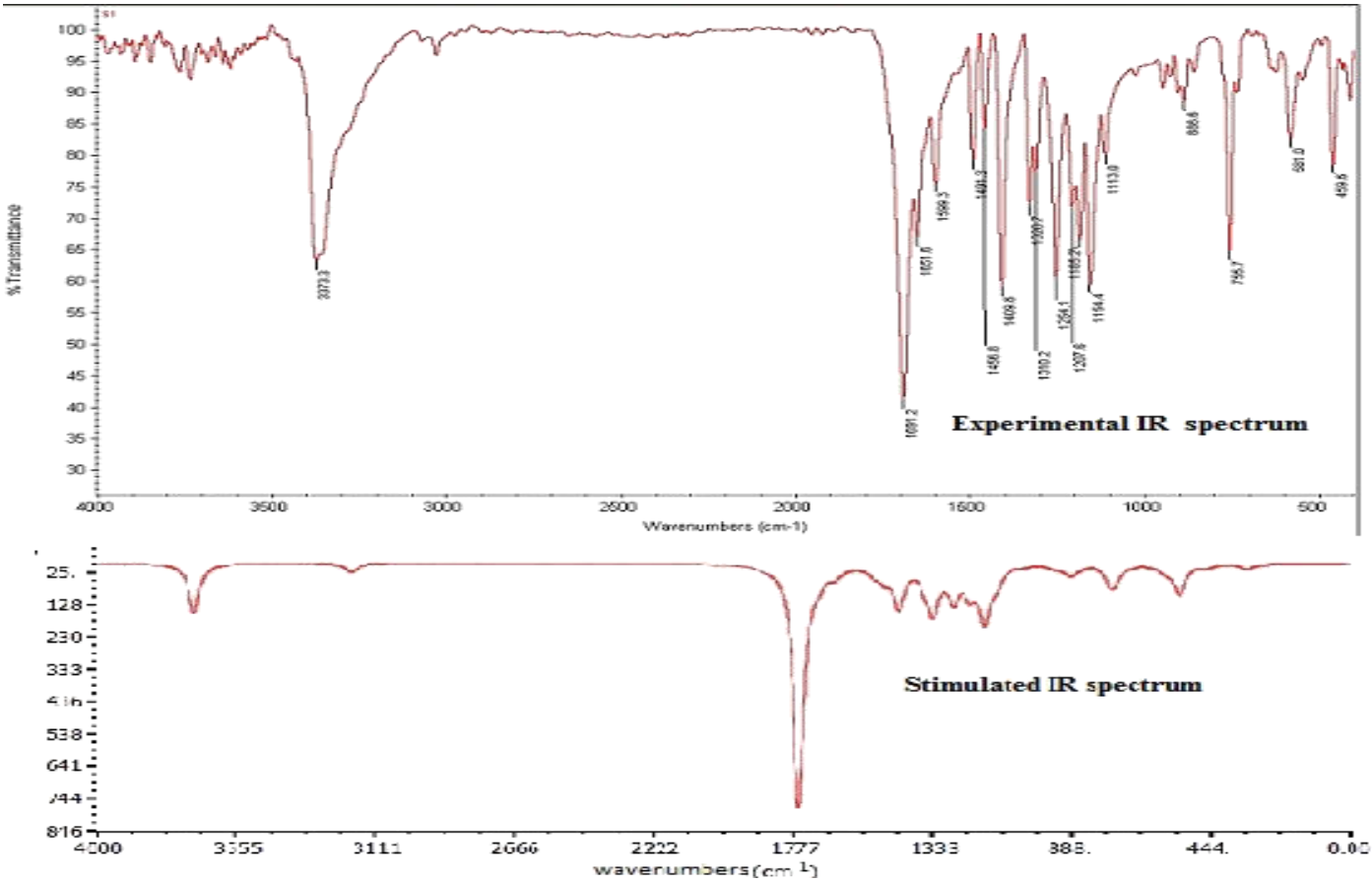

Fig. 4: Experimental and Stimulated FT IR spectra

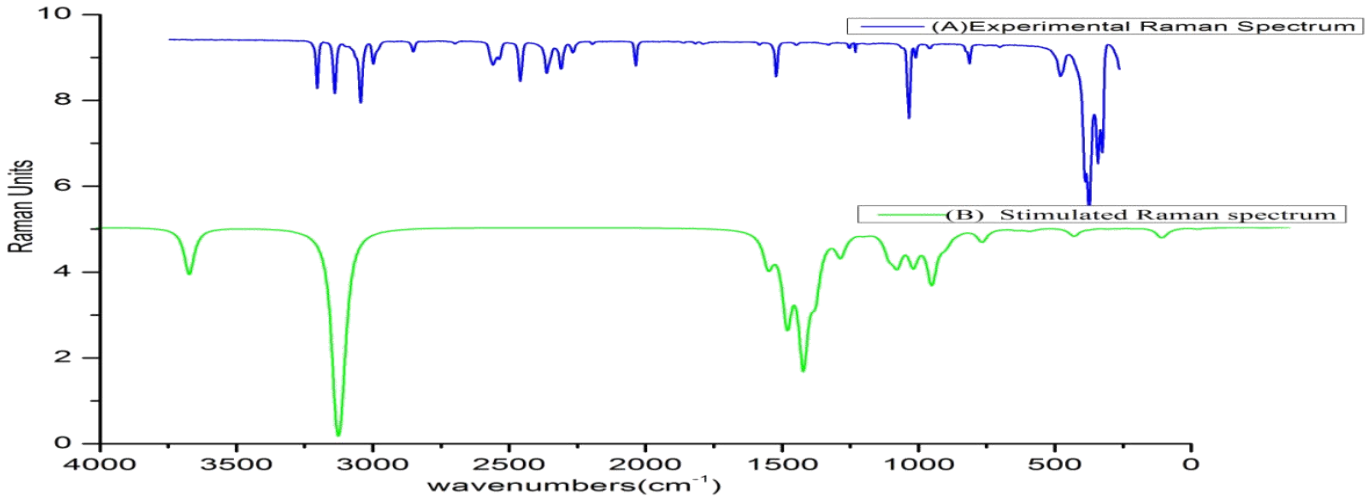

Fig. 5: Experimental and Stimulated Raman spectra

Table 4: Experimental and theoretical B3LYP/6311++G (d,p) IR and RAMAN frequency of 3-hydroxy coumarin

Sl. No.	Experimental frequency		Theoretical frequency (B3LYP) 6311++G(d,p)		Assignment
	FT-IR	FT-Raman	Unscaled	Scaled	
1.	3373		3691	3377.265	ν OH
2.			3203	2930.745	ν CH
3.			3193	2921.595	ν CH
4.			3187	2916.105	ν CH
5.			3181	2910.615	ν CH
6.			3170	2900.55	ν CH
7.	1691	1691	1762	1612.23	ν C=O
8.	1599	1654	1699	1554.585	ν C-O
9.	1491	1601	1645	1505.175	ν C-O
10.	1456	1574	1605	1468.575	ν C-O
11.	1410	1491	1520	1390.8	ν C=C
12.			1488	1361.52	ν C=C
13.	1320	1324	1442	1319.43	ν C=C
14.			1359	1243.485	ν C=C
15.	1310		1332	1218.78	ν C-C
16.		1268	1278	1169.37	ν C-C
17.	1254		1268	1160.22	ν C-C
18.	1207	1213	1217	1113.555	ν C-C
19.	1185	1183	1197	1095.255	ν C-C
20.			1178	1077.87	β OH
21.	1154	1159	1168	1068.72	β CH
22.	1113		1133	1036.695	β CH
23.		1028	1049	959.835	β CH
24.	887		983	899.445	β CH
25.			956	874.74	β CH
26.			933	853.695	β C=O
27.			896	819.84	β C-O
28.			886	810.69	δ OH
29.	756		863	789.645	δ CH
30.			764	699.06	δ CH
31.			750	686.25	δ CH
32.		735	742	678.93	δ CH
33.			725	663.375	δ CH
34.			693	634.095	δ C-O
35.	581		632	578.28	β COH
36.			594	543.51	β CCC
37.			558	510.57	β CCC
38.			544	497.76	β CCC
39.	460		468	428.22	β CCC
40.		459	454	415.41	β CCO
41.			441	403.515	β COC
42.			405	370.575	δ CCC
43.		333	334	305.61	δ CCC
44.			326	298.29	δ CCC
45.			284	259.86	δ CCC
46.			246	225.09	δ CCO
47.		142	112	102.48	δ COC
48.		85	106	96.99	δ COC

3.4.1. OH Vibrations

There is single OH group attached with pyrone rings, whose vibrational frequency is expected in between 3700-3300 cm^{-1} [16]. The scaled value computed using B3LYP function with 6-311++G (d,p) basis set lie at 3377 cm^{-1} and the experimental value at 3373cm^{-1} [17] which clearly shows the presence is hydrogen bond through OH is not favoured, as the wave number value is in lower cut off value.

OH in-plane bending band is expected at 1100 cm^{-1} [18], this is observed at 1077 cm^{-1} in FT-Raman in the present molecule and that of out of plane modes are expected between 710-517 cm^{-1}, but this is observed at 810 cm^{-1} in the present case. This deviation is generally expected at the out of plane modes, as the interaction between various modes at this lower range is very stronger.

3.4.2. C-H Vibrations

For all the aromatic compounds, the carbon-hydrogen stretching vibrations are expected in the region 3100-3000 cm^{-1} and for aliphatic compounds in the region 3000-2900 cm^{-1} [19]. In the present molecule, there are five CH stretching vibrations, in which three belong to benzene ring and the rest belong to pyrone ring. The CH stretching bands which belong the phenyl rings are observed at 2930, 2921 and 2916 cm^{-1}, and that of pyrone ring at 2910 and 2900 cm^{-1} theoretically. These observations indicate that the electronic distribution or conjugation within the benzene rings is altered around the third CH bond. The values at the pyrone ring clearly indicate that the conjugation is completely different within the ring due to O.

The CH bending modes are expected in the range 1300-1000 cm^{-1} and 1000-750 cm^{-1}, respectively for benzene derivatives [20]. In the present case, the in-plane bending bands of benzene and pyrone CH are observed at 1068, 1036, 959, 899 and 874 cm^{-1}. All these values are lesser than the expected range. The out–of- plane modes of the benzene and pyrone are observed at 789, 699, 686, 678 and 663 cm^{-1} in theoretically. Hence, the presence of too many C-O and CC modes in this molecule, which also lie in this range, has pushed down the bending vibrations below the expected range, due to the Fermi resonance effect. The computed values are found closer to the observed values.

3.4.3. C=C, C-C Vibrations

The CC double bond and single bond stretching vibrations are usually expected between1600 to 1500 and 1500 to 1400 cm^{-1} [21] respectively. Though, there used to be no clear cut demarcation between single and double bond within the ring, the higher part of the region is usually assigned to CC double bond stretching modes and the lower part to CC single bond. In present study, the CC double bond stretching is observed at 1390, 1361, 1319 and 1243 cm^{-1} in theoretically. The first two values are quite unusual for benzene ring; they should be assigned to the pyrone ring where the aromaticity like in benzene is not observed.

The CC single bond stretching modes are found at 1218, 1169, 1169, 1160, 1113 and 1095 cm^{-1} in both FT-IR and FT-Raman. According to the structure, double bond CC clearly lies in the expected range. This decrease in values might be due to Fermi resonance and also due to CO modes in this molecule which interfere with these modes.

3.4.4. C=O, C-O Vibrations

For benzene derivatives, the CO double bond and CO single bond stretching vibrations, known as semicircle stretching of hexagonal structure, are usually observed around 1750-1700 cm^{-1} [22-25]. The Stretching vibration for this CO double bond in the present case is observed at 1612 cm^{-1}. The stretching modes of the CO single bonds are expected around 1200-1000 cm^{-1}. In the present case, the stretching vibrations for these CO single bond are observed at 1554, 1505 and 1468 cm^{-1} respectively. All these bonds are present within the pyrone ring, and they almost close to the expected values, which indicate these bands, are not much influenced by the Ketone group present with this ring.

3.5. NBO Analysis

NBO analysis is an important tool for studying hybridization and occupancy effects [26]. Here for the title molecule the NBO analysis was performed using B3LYP/6-311++(d,p) method. This analysis provides a useful method to study inter and intra molecular attraction among the bond pairs. The electron donor orbital, acceptor orbital and interaction stabilization energy are tabulated in Table 5. For each donor and acceptor, the strength of various types of interactions or stabilization energy E^2 associated with electron delocalization between donor and acceptor is estimated by the second-order energy lowering equation [27].

In title compound, it is observed the most probable electronic transitions are found in pyrone ring $n \rightarrow \pi^*$ transitions between the adjacent O atoms and the ring. The second most favoured transitions are $\pi \rightarrow \pi^*$

transitions in the phenyl ring between the C - C bonds. The top most probable electronic transitions were observed: O16 to C5 - O15 (30.6 Kcal/mol n → π*), O15 to C5 - O16 (28.1 Kcal/mol n → π*), O15 to C3-C4 (19.6 Kcal/mol n → π*), O17 to C1-C2 (17.5 Kcal/mol n → π*), C1-C2 to C5-O16 (16.9 Kcal/mol π → π*), O16 to C1-C5 (14.1 Kcal/mol n → π*). All these transitions are taking place within the pyrone ring surrounding the O15, O16 and O17 oxygen atoms. However, only those transitions among them which obey the selection rule and only can appear in the UV-Vis spectrum within the specified wavelength limit, which can also be analyzed theoretically by computing the oscillator strength and absorption coefficients as seen in UV-Visible section.

3.6. UV Analysis

The electronic transition of compound is found out using time-dependent DFT calculations in gas and solvent phases. The calculated results consist of excitation energies (E), oscillator strength (f), and absorption wavelengths which are presented in Table 6. The oscillator strength values are the indicator of the intensity of the peaks in the UV spectrum. The oscillator strength value and HOMO-LUMO contribution values combined will indicate the most favoured transitions among other probable transitions [28]. As seen from the fig. 7, the theoretical electronic absorption spectrum show two peaks at 305 and 206nm, having energy gaps 4.063 & 5.931 eV with oscillator strength of 0.4227 &0.2372 respectively, the corresponding peaks in experimental spectrum are found at 342 and 269 nm respectively illustrated in fig. 6. This transition is corresponds to heterocyclic ring and such interactions between n and π electrons can cause shift in the primary and secondary absorption bands in aromatic compounds. The n → π* transition allows the formation of charge, so the molecular system becomes deficient in electrons while π* system acquires an extra electron causing a separation of charge in the molecule and stabilizing the π* orbitals. The wide gap between the theoretical and experimental values indicate that a large correction factor is required in theory at n → π* transitions.

Table 5: Second Order perturbation theory analysis of Fock matrix in NBO basis for 3-hydroxy coumarin by B3LYP/6-311++G (d,p) method

Donor(i)	Type	ED/e	Acceptor(j)	Type	ED/e	$E^{(2)}$ (Kj/Mol)	E(j)-E(i) (a.u)	F(i,j) (a.u)
O16 (2)	n	1.982	C5 - O15	π *	0.034	30.6	0.51	0.113
O15 (2)	n	1.772	C5 - O16	π*	0.261	28.1	0.33	0.087
O15 (2)	n	1.772	C3 - C4	π*	0.021	19.6	0.38	0.078
O17 (2)	n	1.911	C1 - C2	π*	0.167	17.5	0.36	0.072
C1 - C2	π	1.837	C5 - O16	π*	0.261	16.9	0.28	0.063
O16 (2)	n	1.982	C1 - C5	σ*	0.075	14.1	0.62	0.085
C8 - C11	π	1.827	C3 - C4	π*	0.021	10.9	0.3	0.052
C8 - C11	π	1.827	C9 - C10	π*	0.008	10.8	0.3	0.051
C9 - C10	π	1.821	C3 - C4	π*	0.021	10.8	0.3	0.052
C9 - C10	π	1.821	C8 - C11	π*	0.009	10.4	0.31	0.051
C3 - C4	π	1.758	C1 - C2	π*	0.167	10.1	0.31	0.051
C3 - C4	π	1.758	C8 - C11	π*	0.009	9.88	0.32	0.051
C1 - C2	π	1.837	C3 - C4	π*	0.021	9.77	0.32	0.052
C3 - C4	π	1.758	C9 - C10	π*	0.176	9.61	0.32	0.05
C2 - C3	σ	1.966	C1 - O17	σ*	0.025	5.88	0.89	0.065
O17 (1)	n	1.973	C1 - C5	σ*	0.075	5.78	0.97	0.068
C3 - C8	σ	1.968	C4 - O15	σ*	0.034	5.67	0.87	0.063
C11 - H14	σ	1.981	C3 - C8	σ*	0.023	5.33	0.92	0.063
C10 - H13	σ	1.981	C4 - C9	σ*	0.027	5.31	0.91	0.062
C9 - H12	σ	1.978	C10 - C11	σ*	0.021	5.21	0.93	0.062
H6 - C8	σ	1.979	C10 - C11	σ*	0.021	5.07	0.93	0.061
C2 - H7	σ	1.979	C1 - C5	σ*	0.075	4.71	0.89	0.059
C5 - O16	π	1.994	C1 - C2	π*	0.167	4.63	0.4	0.04

C4 - C9	σ	1.974	C2 - C3	σ*	0.021	4.45	1.02	0.06
O15 (1)	n	1.965	C1 - C5	σ*	0.075	4.39	0.96	0.058
O15 (1)	n	1.965	C3 - C4	σ*	0.021	4.17	1.21	0.064
C2 - C3	σ	1.966	C4 - C9	σ*	0.027	3.62	1.01	0.054
C1 - C5	σ	1.979	C2 - H7	σ*	0.011	3.32	1.12	0.055
C10 - C11	σ	1.978	H6 - C8	σ*	0.011	3.22	1.08	0.053
C10 - C11	σ	1.978	C9 - H12	σ*	0.011	3.07	1.08	0.052
C4 - C9	σ	1.974	C3 - C4	σ*	0.021	2.87	1.24	0.053
C3 - C8	σ	1.968	C3 - C4	σ*	0.021	2.79	1.23	0.052
C3 - C8	σ	1.968	C11 - H14	σ*	0.011	2.79	1.09	0.049
C9 - C10	σ	1.982	C4 - O15	σ*	0.034	2.71	0.99	0.046
O17 - H18	σ	1.985	C1 - C2	σ*	0.016	2.67	1.36	0.054
C4 - C9	σ	1.974	C10 - H13	σ*	0.011	2.62	1.1	0.048
H6 - C8	σ	1.979	C3 - C4	σ*	0.021	2.61	1.14	0.049
C2 - H7	σ	1.979	C3 - C4	σ*	0.021	2.41	1.15	0.047
C5 - O15	σ	1.985	C4 - C9	σ*	0.027	2.39	1.22	0.048
C3 - C4	σ	1.981	C4 - C9	σ*	0.027	2.36	1.14	0.046
C4 - O15	σ	1.985	C3 - C8	σ*	0.023	2.29	1.24	0.048
C9 - H12	σ	1.978	C3 - C4	σ*	0.021	2.23	1.14	0.045
C3 - C4	σ	1.981	C3 - C8	σ*	0.023	2.16	1.15	0.045
C1 - C5	σ	1.979	C1 - C2	σ*	0.016	2.15	1.29	0.047

Table 6: UV analysis of 3-hydroxy coumarin

Gas Phase				Ethanol				
λ (nm)	E(eV)	(f)	Major contribution	Theo. λ (nm)	Exp. λ nm)	E(eV)	(f)	Major contribution
296.9	4.17	0.3281	H→L (93%)	305.1	342	0.4227	4.063	H→L (96%)
278.3	4.45	0.0136	H-1→L (78%)	283.1	269	0.0078	4.380	H-1→L (87%)
247.2	5.01	0.0000	H-2→L (95%)	243.4		0.0274	5.091	H-1→L (10%)
245.0	5.06	0.0178	H-1→L (16%)	237.7		0.0000	5.215	H-3→L (95%)
231.2	5.36	0.0597	H-3→L (10%)	231.1		0.0827	5.362	H-2→L (12%)
223.7	5.54	0.0019	H→L+3 (89%)	222.6		0.0001	5.567	H→L+3 (91%)
216.6	5.72	0.0021	H→L +3(10%)	212.1		0.0061	5.844	H→L +4(90%)
207.2	5.98	0.0011	H→L +5(91%)	209.1		0.2372	5.931	H-2→L (52%)
206.7	5.99	0.2103	H-3→L (52%)	204.8		0.1421	6.051	H-1→L+2(73%)
204.1	6.07	0.0946	H-3→L+1 (11%)	201.5		0.0006	6.151	H→L+5 (96%)

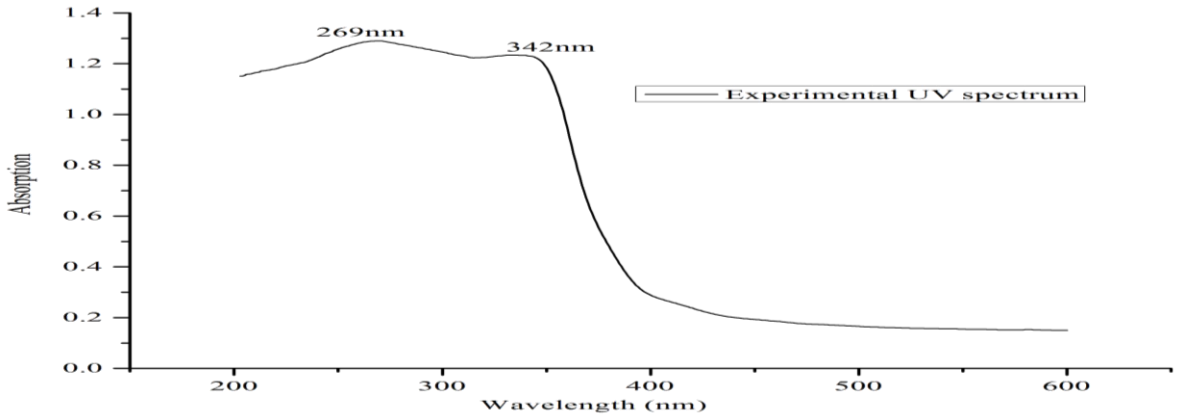

Fig. 6: Experimental UV Spectrum of 3 Hydoxy coumarin

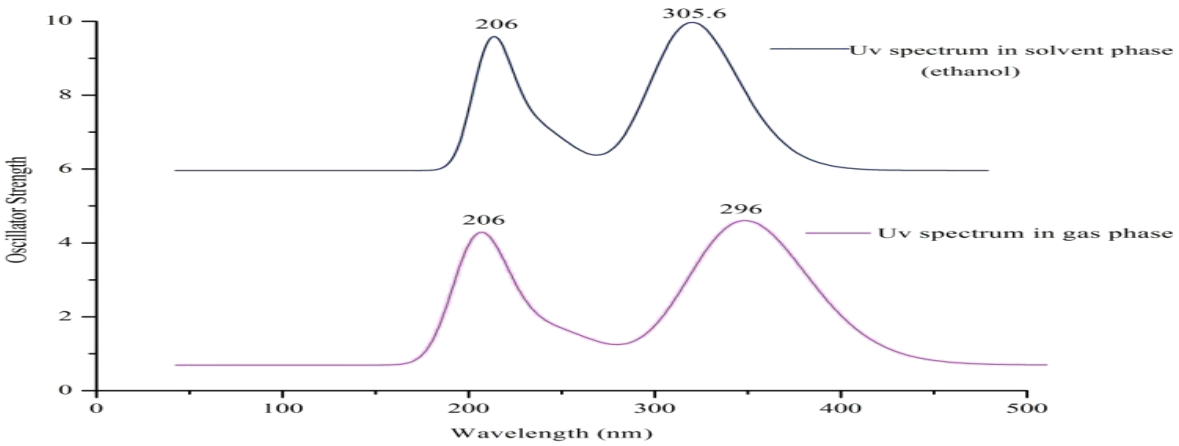

Fig. 7: Stimulated UV Spectrum in gas phase and Solvent phase

3.7. Frontier molecular Orbital's

The Frontier Molecular Orbital (FMO) parameters [29] are the highest occupied molecular orbital (HOMO) and the lowest unoccupied molecular orbital (LUMO) which plays an important role in the chemical stability for the present molecule. HOMO represents the ability to donate an electron and LUMO represent the ability to accept an electron. The FMO parameters are calculated using B3LYP/6-311++G (d, p) basis sets and it is represented in fig. 8. The HOMO → LUMO transition represents the transition of electron density from one atom to another and its transition energies are shown in the Table.7.

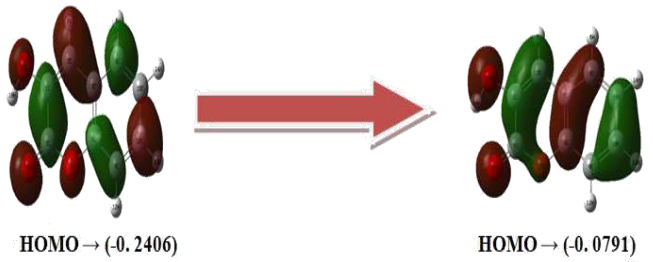

Fig. 8: HOMO-LUMO analysis of 3-hydroxy coumarin

HOMO and LUMO energies are predicted as -0.2406 and -0.0791 a.u. The energy gap between HOMO and LUMO of the present molecule is -0.1615eV which explains the eventual charge transfer interaction that takes place within the molecule and makes the material to be chemical hardness of 0.5636 eV respectively.

The reactivity descriptors such as the global softness and hardness depict the reactivity nature of the molecule. The global softness of the molecule is found to be higher comparatively signifies the molecule has the character of readiness to react to the surrounding nature. In contrast to it the global hardness is very low depicting the less stable nature of the molecule. The electrophilicity index denotes the global electrophilic nature of the molecule and that is comparatively higher and significantly confirming the values of softness.

Table 7: Homo, Lumo, Kubo gap, Global electronegativity, global hardness and softness, gobal electrophilicity index of 3-Hydroxy coumarin

Parameters	Gas
E_{HOMO} (ev)	-0.2406
E_{LUMO} (ev)	-0.0791
$\Delta E_{HOMO-LUMO\ gap}$ (ev)	-0.1615
Electro negativity (χ)	-0.4021
Global hardness (η)	0.5636
Global softness (S)	-0.9657
Chemical potential	1.5293

3.8. Molecular Electrostatic Potential

Molecular Electrostatic Potential (MEP) [30] is mainly used to predict the reactive sites of electrophilic and nucleophilic attack for the title molecule. MEP is obtained at B3LYP/6-311++G(d,p) basis sets and shown in fig. 9. It shows the 3D-electrostatic potential map of the title molecule. This mapping visualizes the distribution of charged regions which is used to determine the interaction of molecules with one another. In this contour mapping, the different colors red, blue and green represent the most negative, most positive and zero electrostatic potential regions. From the MEP surface of the title molecule, it is observed that

the negative charges cover the C=O group, OH group and the positive charge covers over the benzene ring. The color code of the mapping surface is in the range between -4.922 a.u. (deepest red) and 4.922 a.u (deepest blue). The negative potential is due to π charges and it is more prone to electrophilic attack. The positive region may be considered as barrier to electrophilic attack. From this result, it is clear that the benzene ring indicates the strongest attraction and the C=O group, OH hydroxyl group indicate the strongest repulsion.

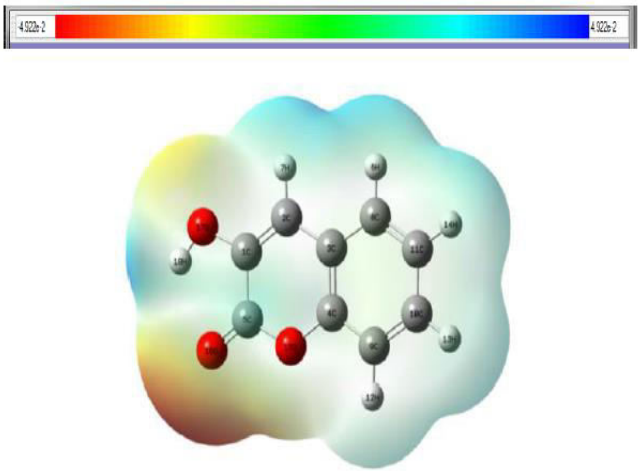

Fig. 9: MEP pictorial of 3-Hydroxy Coumarin

3.9. Docking Analysis

Molecular Docking is a significant tool used in computer aided drug design.Autodock software package [31-32] is utilized to perform docking simulation. Autodock is a suite of automated docking tools. It is designed to specify how small molecules bind to a receptor of known 3D structures. Graphical user interface is used to find the protein structures of the ligand. Lamarckian genetic Algorithm (LGA) was utilized in molecular docking calculation.

The Auto Dock Bonded distance, bonded residue and hydrogen bond lengths are shown in the Table 8. Potential problems such as added waters, missing atom, chain breaks etc., are avoided before in ADT using Python Molecular Viewer. In the analysis, it is found that the receptor is the protein 5dbq and the title compound binds to the receptor at three sites which are named as residues.

The optimized structure of the compound was docked to the protein through the hydrogen bond at all the three oxygen atoms with bond lengths t 1.9 A , 2.2 A and 3.0 A are depicted in fig. 10. From the docking analysis and resultant parameters, the molecule under investigation can be considered as a potential anti-bacterial drug and it can be used in drug designing in near future studies.

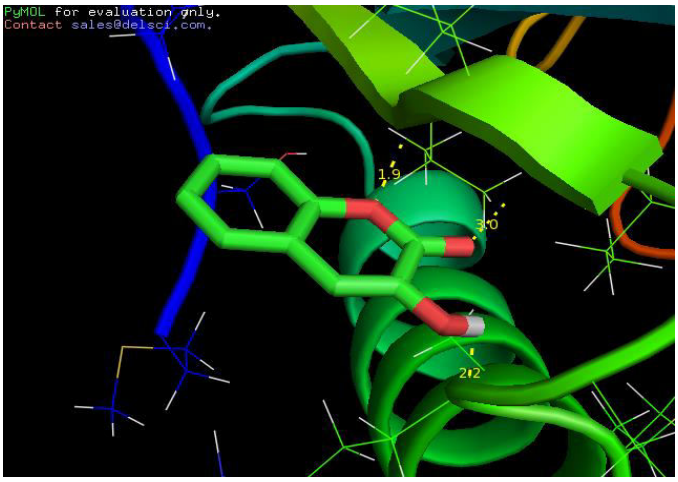

Fig. 10: Molecular docking analysis of 3-Hydroxy coumarin

Table 8: Docking analysis of 3-hydroxy coumarin

Protein ID	Bonding energy	Bond Residue	Distance (Å)
5dbq	4.95	VAL 55	1.9
		VAL 55	2.2
		ALA 46	3.0

4. CONCLUSION

The variation in bond lengths in the structural analysis shows that there is no conjugation of electrons in the pyrone ring as it is used to be in phenyl rings. From Mullikan charge analysis, it is observed that, in benzene ring, all carbon atoms have almost negative charges and they are ready to interact with the positive charge acceptors. C1 which lies in the hydroxyl group has equally large shift because of the Oxygen atom. The NAC methods of charge distribution among these carbon atoms support these chemical shift values. The UV transitions among them obey the selection rule and only they appear in the UV-Vis spectrum within the specified wavelength limit, which can also be analyzed theoretically by computing the oscillator strength and absorption coefficients as seen in UV-Visible section. It is clear that the benzene ring indicates the strongest attraction and the C=O group, OH hydroxyl group indicate the strongest repulsion. From the result of

docking studies, the title molecule 3HC has significant anti-bacterial activity.

Conflict of interest

None declared

5. REFERENCES

1. Li JW- H, Vederas JC et al. *Science,* 2009; **325(80):**161-165.
2. Rodrigues T, Reker D, Schneider P, Schneider G. *Nat Chem.* 2016; **8**:531-541.
3. Sharma V K, Saharo P D, Sharma N, Rastogi R C. *Spectrochim. Acta A*., 2003; **59:**1161-1170.
4. Yu X, Scheller D, Rademacher O, Wolff T. *J. Org. Chem.*, 2003; **68**:7386-7399.
5. Wei H, Ruan J, Zhang, et al., *RSC Adv*., 2016; **6**:10846-10860.
6. Behl C. *Cell Tissue Res*., 1997; **29**:471.
7. Frisch MJ, Trucks GW, Schlegal HB, Scuseria GE, Robb MA, et al., Gaussian09, Revision A. 02, *Gaussian, inc*., Wallingford CT, 2009.
8. Xavier S, Sebastian S. et al. *journal of Molecular structure,* 2016; **1125**:204-216.
9. Shoba D, Boomadevi S. et al. *Spectrochimica Academic Press*, 2000.
10. Ramalingam S, Karabavak M. et al. *Spectrochimica Acta Part A*, 2012; **94**: 318-330.
11. Mulliken RS, *J. Chem. Phys*., 1995; **23**:1840-1883.
12. Thilagavathi G, Arivazhagan M, *J.Spectrochim. Acta A*, 2010; **79**:389-395.
13. Karthick T, Balachandran V, Perumal S*, J of mol. St*., 2011; **1005**:202-213.
14. Ismail Kul, Krishna Bhat, Megan Hums, Michael Miller, SevilSener, *J of fluid phase equilibria*, 2013; **351**:94-104.
15. Robert Uhrecky, JauPavlik, ZdeukaRuzickova, LuborDlhan, Marian Koman, Roman Boca, et al. *J of mol structure,* 2014; **1076**:10-19.
16. Michela A, Danilo S, Valentina G, Giuseppe V, Roberto DC, Raffaele M. *Applied catalysis A: General*, 2014; **487**:91-99.
17. Chi-Hui Tson, Hsun-Tsing Lee, Wei-Song Hung, Chyung-Chyung Wang, Chia-Chen Chu, Maw-CherngSuen, et al. *polymer*, 2016; **85**:96-105.
18. Sedat Y, Sadiye OY, Sidika C, Oguzhan A, Pinar Y, Levent O. *Applied catalysis B: Environmental*, 2017; **202**:500-508.
19. Sharma YR, *Elementry Oraganic Spectroscopy, revised ed*., S. Chand, New Delhi, 2013; 204.
20. Arjunan V et al. *J Spectrochem Acta Part A: Mol. Biomospectrosc.,* 2012; **96**:506-516.
21. Prabakaran A, Muthu S. *J Spectrochem, Acta Part A: Mol. Biomol. Spectrosc*., 2014; **118**:578-588.
22. Jayasheela K, Periandy S, Xavier S, Niveditha K, *Intern. J. of Research on Eng., and Tech.,* 2018.
23. Ramaekers R, Maes G, Adamowicz L, Dkhissi A, *J. Mol. Struct.,* 2001;**560**:205-221.
24. Gunasekaran S, Natarajan RK, Rathikha R, Syamala D, *Ind. J. Pure Appl. Phys*., 2005; **43**:503.
25. Ramalingam S, Periandy S, Govindarajan M, Mohan S, *Spectrochim. Acta Part A*, 2010; **75**:1552-1558.
26. Almutairi S, Jayasheela K, Periandy S, Alwah. Al-Ghamdi R, et al*., J. Mol. Struct,* 2019; **1196**:578-591.
27. Sundaraganesan N, Uma MH, Dominic JB, Meganathan C, Ramalingam M. *J. Mol. Structure (Theo chem.),* 2008; **850**:84-93.
28. Muthu S, Paulraj EI. *J.Chem.Pharm. Res*., 2011; **3(5):**323-339.
29. Murray JS, Sen K. *Molecular Electrostatic Potentials, Concepts and Applications*, Elsevier, Amsterdam, 1996; 399.
30. Moorthy N et al. *J of Molstruct*, 2016.
31. Arokiasamy A, Manikandan G et al. *J of Molstruct,* 2017. DOI: 10.1016/j/ molstruc.2016.12.051.
32. Madanagopal A, Periandy S, et al, *Journal for Science,* 2017. DOI: 10.1016/j.jtusci.2017. 02.006